First Measurements of the Double-Polarization Observables F, P, and H in ω Photoproduction off Transversely Polarized Protons in the N^* Resonance Region

P. Roy,[14,*] S. Park,[14,†] V. Crede,[14,‡] A. V. Anisovich,[3,49] E. Klempt,[3] V. A. Nikonov,[3,49] A. V. Sarantsev,[3,49] N. C. Wei,[48,50] F. Huang,[50] K. Nakayama,[17] K. P. Adhikari,[34,§] S. Adhikari,[13] G. Angelini,[16] H. Avakian,[40] L. Barion,[19] M. Battaglieri,[21] I. Bedlinskiy,[26] A. S. Biselli,[11] S. Boiarinov,[40] W. J. Briscoe,[16] J. Brock,[40] W. K. Brooks,[41] V. D. Burkert,[40] F. Cao,[9] C. Carlin,[40] D. S. Carman,[40] A. Celentano,[21] P. Chatagnon,[24] T. Chetry,[33] G. Ciullo,[12,19] P. L. Cole,[18,29] M. Contalbrigo,[19] O. Cortes,[16] A. D'Angelo,[22,36] N. Dashyan,[47] R. De Vita,[21] E. De Sanctis,[20] A. Deur,[40] S. Diehl,[9] C. Djalali,[33,38] M. Dugger,[2] R. Dupre,[1,24] B. Duran,[39] H. Egiyan,[31,40] M. Ehrhart,[24] A. El Alaoui,[41] L. El Fassi,[30] P. Eugenio,[14] S. Fegan,[42] A. Filippi,[23] A. Fradi,[24,¶] G. P. Gilfoyle,[35] F. X. Girod,[7,40] E. Golovatch,[37] R. W. Gothe,[38] K. A. Griffioen,[46] M. Guidal,[24] L. Guo,[13,40] K. Hafidi,[1] C. Hanretty,[14,40] N. Harrison,[40] M. Hattawy,[34] T. B. Hayward,[46] D. Heddle,[8,40] K. Hicks,[33] M. Holtrop,[31] Y. Ilieva,[16,38] D. G. Ireland,[42] B. S. Ishkhanov,[37] E. L. Isupov,[37] D. Jenkins,[44] H. S. Jo,[28] S. Johnston,[1] S. Joosten,[39] M. L. Kabir,[30] C. D. Keith,[40] D. Keller,[45] G. Khachatryan,[47] M. Khachatryan,[34] A. Khanal,[13] M. Khandaker,[32,**] A. Kim,[9] W. Kim,[28] F. J. Klein,[6] V. Kubarovsky,[40] S. V. Kuleshov,[26,41] M. C. Kunkel,[25] L. Lanza,[22] P. Lenisa,[19] K. Livingston,[42] I. J. D. MacGregor,[42] D. Marchand,[24] B. McKinnon,[42] D. G. Meekins,[40] C. A. Meyer,[5] T. Mineeva,[41] V. Mokeev,[37,40] R. A. Montgomery,[42] A Movsisyan,[19] C. Munoz Camacho,[24] P. Nadel-Turonski,[40] S. Niccolai,[24] G. Niculescu,[27] M. Osipenko,[21] A. I. Ostrovidov,[14] M. Paolone,[39,38] L. L. Pappalardo,[19] R. Paremuzyan,[31,47] E. Pasyuk,[40] D. Payette,[34] W. Phelps,[16] J. Pierce,[45,††] O. Pogorelko,[26] Y. Prok,[8,34,45] D. Protopopescu,[42] B. A. Raue,[13,40] M. Ripani,[21] D. Riser,[9] B. G. Ritchie,[2] A. Rizzo,[22,36] G. Rosner,[42] F. Sabatié,[7] C. Salgado,[32] R. A. Schumacher,[5] M. L. Seely,[40] Y. G. Sharabian,[40] U. Shrestha,[33] Iu. Skorodumina,[37,38] D. Sokhan,[42] O. Soto,[41] N. Sparveris,[39] I. I. Strakovsky,[16] S. Strauch,[38] M. Taiuti,[15,‡‡] J. A. Tan,[28] B. Torayev,[34] N. Tyler,[38] M. Ungaro,[9,40] H. Voskanyan,[47] E. Voutier,[24] N. K. Walford,[6] R. Wang,[24] D. P. Watts,[43] X. Wei,[40] M. H. Wood,[4] N. Zachariou,[16,43] J. Zhang,[34,45] and Z. W. Zhao[10,38,45]

(CLAS Collaboration at Jefferson Lab)

[1] *Argonne National Laboratory, Argonne, Illinois 60439, USA*
[2] *Arizona State University, Tempe, Arizona 85287-1504, USA*
[3] *Helmholtz-Institut für Strahlen- und Kernphysik, Universität Bonn, 53115 Bonn, Germany*
[4] *Canisius College, Buffalo, New York 14208, USA*
[5] *Carnegie Mellon University, Pittsburgh, Pennsylvania 15213, USA*
[6] *Catholic University of America, Washington, D.C. 20064, USA*
[7] *IRFU, CEA, Université Paris-Saclay, F-91191 Gif-sur-Yvette, France*
[8] *Christopher Newport University, Newport News, Virginia 23606, USA*
[9] *University of Connecticut, Storrs, Connecticut 06269, USA*
[10] *Duke University, Durham, North Carolina 27708-0305, USA*
[11] *Fairfield University, Fairfield CT 06824, USA*
[12] *Università di Ferrara, 44121 Ferrara, Italy*
[13] *Florida International University, Miami, Florida 33199, USA*
[14] *Florida State University, Tallahassee, Florida 32306, USA*
[15] *Università di Genova, 16146 Genova, Italy*
[16] *The George Washington University, Washington, DC 20052, USA*
[17] *University of Georgia, Athens, GA30602, USA*
[18] *Idaho State University, Pocatello, Idaho 83209, USA*
[19] *INFN, Sezione di Ferrara, 44100 Ferrara, Italy*
[20] *INFN, Laboratori Nazionali di Frascati, 00044 Frascati, Italy*
[21] *INFN, Sezione di Genova, 16146 Genova, Italy*
[22] *INFN, Sezione di Roma Tor Vergata, 00133 Rome, Italy*
[23] *INFN, Sezione di Torino, 10125 Torino, Italy*
[24] *Institut de Physique Nucléaire, IN2P3-CNRS, Université Paris-Sud, Université Paris-Saclay, F-91406 Orsay, France*
[25] *Institute für Kernphysik, 52425 Jülich, Germany*
[26] *Institute of Theoretical and Experimental Physics, Moscow, 117259, Russia*
[27] *James Madison University, Harrisonburg, Virginia 22807, USA*
[28] *Kyungpook National University, Daegu 41566, Republic of Korea*
[29] *Lamar University, 4400 MLK Blvd, PO Box 10009, Beaumont, Texas 77710, USA*
[30] *Mississippi State University, Mississippi State, MS 39762-5167, USA*
[31] *University of New Hampshire, Durham, New Hampshire 03824-3568, USA*
[32] *Norfolk State University, Norfolk, Virginia 23504, USA*

[33] *Ohio University, Athens, Ohio 45701, USA*
[34] *Old Dominion University, Norfolk, Virginia 23529, USA*
[35] *University of Richmond, Richmond, Virginia 23173, USA*
[36] *Università di Roma Tor Vergata, 00133 Rome, Italy*
[37] *Skobeltsyn Institute of Nuclear Physics, Lomonosov Moscow State University, 119234 Moscow, Russia*
[38] *University of South Carolina, Columbia, South Carolina 29208, USA*
[39] *Temple University, Philadelphia, PA 19122, USA*
[40] *Thomas Jefferson National Accelerator Facility, Newport News, Virginia 23606, USA*
[41] *Universidad Técnica Federico Santa María, Casilla 110-V Valparaíso, Chile*
[42] *University of Glasgow, Glasgow G12 8QQ, United Kingdom*
[43] *University of York, York YO10, United Kingdom*
[44] *Virginia Tech, Blacksburg, Virginia 24061-0435, USA*
[45] *University of Virginia, Charlottesville, Virginia 22901, USA*
[46] *College of William and Mary, Williamsburg, Virginia 23187-8795, USA*
[47] *Yerevan Physics Institute, 375036 Yerevan, Armenia*
[48] *Zhengzhou University, Zhengzhou, Henan 450001, China*
[49] *NRC "Kurchatov Institute", PNPI, 188300, Gatchina, Russia*
[50] *School of Nuclear Science and Technology, University of Chinese Academy of Sciences, Beijing 100049, China*
(Dated: Received: May 1, 2019/ Revised version:)

First measurements of double-polarization observables in ω photoproduction off the proton are presented using transverse target polarization and data from the CEBAF Large Acceptance Spectrometer (CLAS) FROST experiment at Jefferson Lab. The beam-target asymmetry F has been measured using circularly polarized, tagged photons in the energy range 1200–2700 MeV, and the beam-target asymmetries H and P have been measured using linearly polarized, tagged photons in the energy range 1200–2000 MeV. These measurements significantly increase the database on polarization observables. The results are included in two partial-wave analyses and reveal significant contributions from several nucleon (N^*) resonances. In particular, contributions from new N^* resonances listed in the Review of Particle Properties are observed, which aid in reaching the goal of mapping out the nucleon resonance spectrum.

PACS numbers: 13.60.Le, 13.60.-r, 14.20.Gk, 25.20.Lj

Photoproduction of the isoscalar vector mesons ω and ϕ off the proton plays an important role in our understanding of many hadronic physics phenomena in the non-perturbative regime. Photoproduction of an ω meson at lower energies provides unique information on the mechanism of nucleon resonance excitation and on the strength of the $\omega N N^*$ coupling, which aids in shedding light on the structure of baryon resonances.

The study of ω-meson photoproduction is particularly interesting in the search for new, hitherto unknown nucleon resonances. The reaction threshold lies above the thresholds for π and η photoproduction and therefore, ω photoproduction probes the higher-mass nucleon states above $W = 1700$ MeV. At these center-of-mass energies, the πN and ηN photoproduction cross sections are significantly smaller. Moreover, the ω meson is an isoscalar particle and is sensitive only to $I = 1/2$ (nucleon) resonances which reduces the complexity of the contributing intermediate states. A discussion of recent progress toward understanding the nucleon resonance spectrum can be found in recent reviews, e.g. Refs. [1, 2].

In this letter, we report on the first measurements of the polarization observables F, P, and H for the reaction

$$\vec{\gamma}\,\vec{p} \to p\,\omega \quad \text{where } \omega \to \pi^+\,\pi^-\,\pi^0\,, \tag{1}$$

using linearly as well as circularly polarized tagged photons and transversely polarized protons. Without measuring any recoil polarization, the differential cross section for this combination is given by [3–5]

$$\begin{aligned}\frac{d\sigma}{d\Omega} = \frac{d\sigma_0}{d\Omega}\,\{\,(\,1 \,-\, \delta_l\,\Sigma\cos 2\beta\,) \\ + \Lambda\cos\alpha\,(-\delta_l\,H\sin 2\beta \,+\, \delta_\odot\,F\,) \\ - \Lambda\sin\alpha\,(-T \,+\, \delta_l\,P\cos 2\beta\,)\,\}\,,\end{aligned} \tag{2}$$

where δ_l ($\delta_\odot$) denotes the degree of linear (circular) beam polarization and Λ denotes the degree of target polarization. For transverse target polarization, the available polarization observables are the target asymmetry T, the beam-target asymmetry F using a circularly polarized beam, and the beam-target asymmetries H and P using a linearly polarized beam. The angle β (α) describes the inclination of the linear-beam (transverse-target) polarization with respect to the center-of-mass plane spanned by the beam axis and the recoil proton.

The FROzen-Spin Target (FROST) experiment, conducted at the Thomas Jefferson National Accelerator Facility, was designed to perform measurements with polarized beams and targets. The details of the experiment are discussed in Refs. [6–8].

The CEBAF accelerator facility at Jefferson Lab delivered longitudinally polarized electrons with energies up to 2.4 GeV and a polarization of about 87 % [9]. Circularly polarized photons were then obtained by transfer-

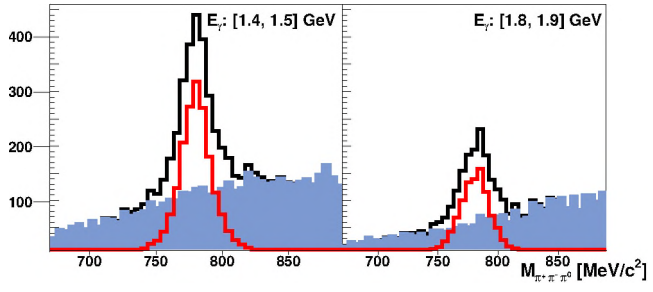

FIG. 1. (Color online) Typical examples of signal and background mass distributions from butanol data after applying all kinematic cuts and corrections. The invariant $\pi^+\pi^-\pi^0$ masses are shown for two energies at the same angle, $0.2 < \cos\Theta^{\omega}_{\rm c.m.} < 0.4$. The **black line** shows the unweighted distribution from the butanol target, the blue-shaded area shows the background mass distribution (weighted by $1-Q$), and the red line shows the signal distribution (weighted by Q.)

ring the polarization from the electrons to the photons in a bremsstrahlung process when the electrons scattered off an amorphous gold radiator. The larger the fractional energy carried by the photon with respect to the electron energy, the greater the degree of polarization [6, 10].

Linearly polarized photons were created via coherent bremsstrahlung by scattering unpolarized electrons off a diamond crystal. These polarized photons typically covered a 200-MeV-wide energy range below the sharp coherent edge. Data were recorded with the position of the coherent edge ranging from 700 MeV to 2100 MeV, in steps of 200 MeV. The degree of linear polarization was determined by fitting the energy distributions of the incident photons and was observed to vary between 40–60 %. The polarized photons were energy and time tagged with resolutions of 0.1 % and 100 ps, respectively, using a photon tagging system [11].

A state-of-the-art component of the experiment was the polarized target, described in detail in Ref. [8]. It was placed at the center of the CLAS spectrometer, and provided an average degree of polarization of 81 %. The direction of the polarization was reversed every 5–7 days. To study background originating from unpolarized protons of the carbon and oxygen atoms in the butanol target, carbon and polyethylene disks were placed at approximately 9 cm and 16 cm downstream of the butanol target. The vertex distribution shows distinct peaks from each target, allowing for a clean separation of events.

The CLAS detector, with its six-fold symmetry about the beamline, was capable of detecting charged particles with a laboratory polar-angle coverage of $[8,\ 142]^\circ$ and almost 2π coverage in the azimuthal angle. The final-state particles traversed several layers of sub-detectors, including drift chambers (DC) and time-of-flight (TOF) scintillators. A start counter (SC) provided the initial time information of the events. Full details of the CLAS detector are provided in Ref. [12]. For an event to be recorded, the trigger conditions required at least one charged particle in the final state.

In this analysis, the ω was reconstructed from its $\pi^+\pi^-\pi^0$ decay, which has the highest branching ratio (89 %) among all ω decay modes. Events were selected to have exactly one incident-photon candidate with a timing (using the photon tagger) at the event vertex within 1 ns of the event time provided by the SC. Only those events that had exactly one proton, plus one positively charged and one negatively charged pion track in the final state were retained. To further improve the particle identification, each final-state particle's β value was calculated separately from its measured momentum using the DC, $\beta_{\rm DC}$, and from its measured velocity using the TOF system and the SC, $\beta_{\rm TOF}$. Events were selected based on good agreement of $\beta_{\rm DC}$ and $\beta_{\rm TOF}$ [7, 9]. The momenta of the final-state particles were corrected for energy losses using standard CLAS techniques. Additional corrections of a few MeV were required for the momentum magnitudes, which are discussed in detail in Refs. [6, 7, 9].

A four-constraint (4C) kinematic fit to the exclusive $\gamma p \to p\,\pi^+\pi^-$ reaction imposing energy and momentum conservation aided in tuning the full covariance matrix. The reaction $\gamma p \to p\,\pi^+\pi^-$ (missing π^0) was next kinematically fit, and events with a confidence level below 0.001 were rejected, removing most of the $\pi^+\pi^-$ background. The remaining background consisted mostly of $p\,\omega$ events originating from unpolarized bound protons in the butanol (C_4H_9OH) target and non-$p\,\omega$ events resulting in a $p\,\pi^+\pi^-\pi^0$ final state. These were accounted for using the Q-factor technique, which determines the probability for an event to be a signal event (as opposed to background) on the basis of a sample of its nearest kinematic neighbors in a very small region of the multi-dimensional $\pi^+\pi^-\pi^0$ phase space around the candidate event [7, 13]. The method assumes that the signal and background distributions do not vary rapidly in the selected region. The $\pi^+\pi^-\pi^0$ mass distribution of each event and its nearest kinematic neighbors was fit using a Voigtian for the signal probability function (pdf) and a third-order Chebychev polynomial for the background pdf. The value of Q is then defined as the ratio of signal amplitude to total amplitude at the mass of the candidate event. Figure 1 shows examples of signal and background distributions in the invariant $\pi^+\pi^-\pi^0$ mass obtained by weighting each event with Q and $1-Q$, respectively.

For each bin in incident-photon energy and meson center-of-mass angle $(E_\gamma, \cos\Theta^{\omega}_{\rm c.m.})$, an event-based maximum-likelihood technique was applied to fit the azimuthal angular distributions of the recoil proton in the lab frame to extract the polarization observables [14]. The likelihood function in each kinematic bin is

$$-\ln L = -\sum_{i=1}^{N_{\rm events}} w_i \ln\left(P_i\right), \quad P_i = \frac{1 \pm A}{2}, \qquad (3)$$

and $A = (N_1 - N_2)/(N_1 + N_2)$ denotes the asymmetry in the azimuthal angular distributions of events with different orientations of the beam-target polarization. The sign of A depends on the corresponding relative orientation of the beam-target polarization in the ith event. The weights, w_i, depend on the Q factors and additional normalization factors. More details and a complete list of definitions are given in Refs. [7, 9].

The asymmetry A depends on the differential cross section (Eqn. 2) and hence, on the polarization observables. Maximizing the likelihood $\mathcal{L}$ gives the most likely values for the observables. Owing to statistical limitations, a simultaneous fit to all polarization observables did not converge. Different data sets, corresponding to the different orientations of the beam-target polarization, were combined with appropriate normalization factors to reduce the number of unknown parameters in the likelihood expression. The observable F was determined separately using circular beam polarization, whereas the observables H and P were determined from simultaneous fits using linear beam polarization (see Eqn. 2).

A major contribution to the overall systematic uncertainty came from the background subtraction. This Q factor uncertainty was determined for all observables in each $(E_\gamma, \cos\,\Theta^{\omega}_{\mathrm{c.m.}})$ bin by modifying each Q factor by its corresponding fit uncertainty σ_Q, and re-extracting the observable. The absolute difference was taken as the systematic uncertainty and averaged about 8 % for incident-photon energies > 1.3 GeV. Other sources of uncertainty included the degree of linear- (circular-) beam polarization (5 % (4 %)), the degree of transverse-target polarization (2 %), the direction of the target polarization (2 %) and the flux normalization. The latter was 5 % for data with linear-beam polarization, and 2 % for data with circular-beam polarization since the beam helicity flipped rapidly leading to the same photon flux for opposite beam helicities. Gray bands in the figures show only absolute systematic uncertainties due to the background subtraction; scale-type uncertainties are not included.

The ω polarization observables presented here are first-time measurements, representing a substantial increase in the world database for ω photoproduction. Figure 2 shows the beam-target asymmetry F and Fig. 3 shows the beam-target asymmetries H and P for the incident-photon energy range 1200–2000 MeV in 100-MeV-wide bins and 10 and 5 $\cos\Theta^{\omega}_{\mathrm{c.m.}}$ bins in the center-of-mass frame, respectively. The asymmetries are substantial and vary significantly with energy, indicative of strong contributions from nucleon resonances.

The role of N^* resonances in ω photoproduction has long been discussed in the literature, e. g., using effective Lagrangian [15–17] and coupled-channel K-matrix approaches [18, 19]. Given the scarcity of data at the time, most of these studies were based only on the differential cross section data, and not surprisingly disagree on the contribution of N^* resonances.

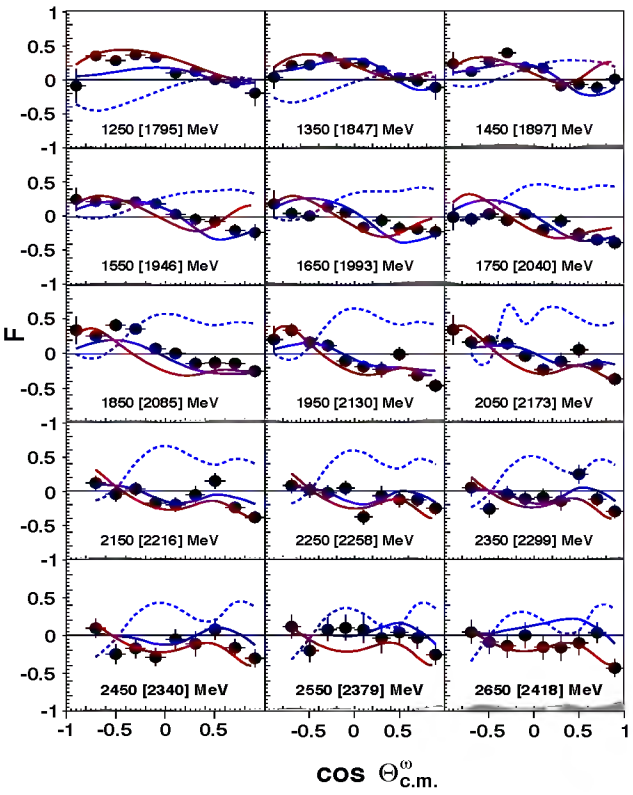

FIG. 2. First-time measurement of the beam-target asymmetry F in $\vec{\gamma}\vec{p} \to p\omega$. Shown are distributions in 100-MeV-wide incident-photon energy bins (labeled as $E_\gamma\,[W]$) as a function of $\cos\Theta^{\omega}_{\mathrm{c.m.}}$ in the center-of-mass frame. Each data point has been assigned its statistical uncertainty, whereas the gray band at the bottom of each panel represents the absolute systematic uncertainties due to the background subtraction. The blue and red solid curves show the BnGa PWA solution and fits by Wei *et al.* [23], respectively. The blue dashed curve denotes an earlier BnGa solution [26].

The data presented here, and further ω data from the FROST experiment on the helicity asymmetry E [6] and on the single-polarization observables Σ [7, 20] and T [7] (beam and target asymmetries, respectively) were included in two independent analyses: A partial-wave analysis (PWA) within the Bonn-Gatchina (BnGa) coupled-channel framework [21] based on a large database of pion- and photon-induced reactions [22], and a tree-level-based effective Lagrangian approach [23], shown in Figs. 2 and 3 as the solid and dashed lines, respectively. In contrast to the coupled, multi-channel BnGa analysis, the effective Lagrangian approach of Ref. [23] considers only the ωN channel. The reaction amplitude consists of s-, t-, and u-channel Feynman diagrams combined with a phenomenological contact current which accounts for effects not explicitly included and is required for local gauge invariance of the overall amplitude. More details are given in Refs. [24, 25].

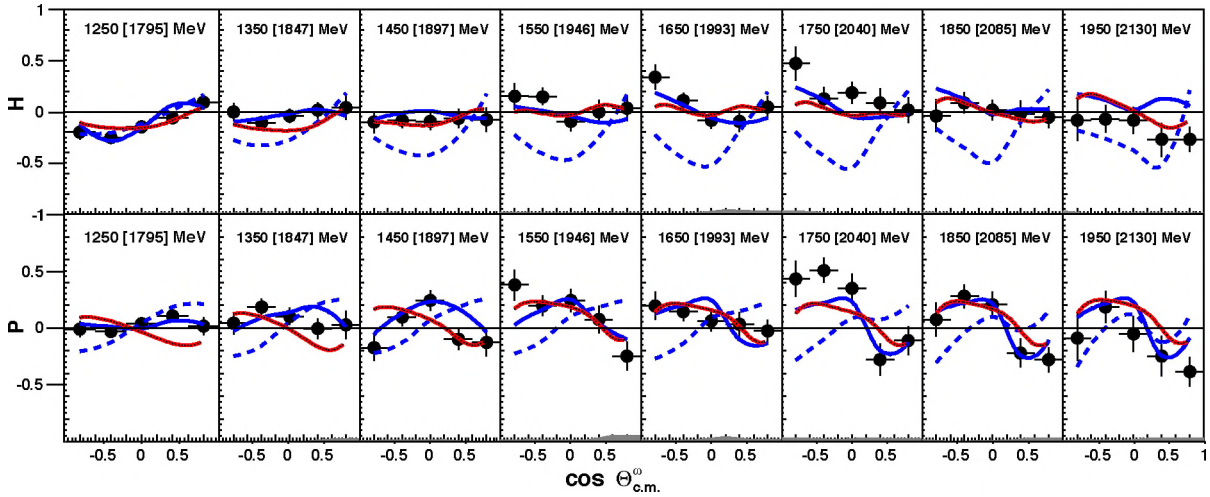

FIG. 3. (Color online) First-time measurements of the beam-target asymmetries H (top) and P (bottom) in ω photoproduction off the proton. Shown are eight 100-MeV-wide energy bins (labeled as $E_\gamma\,[W]$) as a function of $\cos\Theta^{\omega}_{\mathrm{c.m.}}$ in the center-of-mass frame. Each data point has been assigned its statistical uncertainty, whereas the gray band at the bottom of each panel represents the absolute systematic uncertainties due to the background subtraction. The blue and red solid curves show the BnGa PWA solution and fits by Wei *et al.* [23], respectively. The blue dashed curve denotes an earlier BnGa solution [26].

The BnGa description of these new data started with a PWA solution of an earlier analysis that is discussed in Ref. [26]. This initial analysis was based on results in $\gamma p \to p\omega$ ($\omega \to \pi^0\gamma$) obtained by the CBELSA/TAPS Collaboration on differential cross sections [27], the double-polarization observables $\mathbf{G}$, $\mathbf{G}_\pi$ [28], the beam asymmetry Σ [29] and a variety of spin-density matrix elements (SDMEs): ρ^1_{00}, ρ^1_{11}, ρ^1_{1-1}, ρ^1_{10}, ρ^2_{10}, ρ^2_{1-1} (using linear-beam polarization) as well as ρ^0_{00}, ρ^0_{10}, ρ^0_{1-1} (unpolarized beam) [27].

The earlier analysis revealed significant t-channel contributions from the exchange of pomerons, which increase with energy and account for about 50 % of the total cross section at about $W = 2$ GeV. Moreover, the polarization observables and SDMEs revealed notable contributions from as many as 12 nucleon resonances, and several branching ratios were determined for the first time [26]. Evidence was found for the poorly known states $N(1880)\,1/2^+$, $N(2000)\,5/2^+$, $N(1895)\,1/2^-$, and $N(2120)\,3/2^-$. Small contributions were also revealed from several weaker partial waves. However, this solution provided a poor description of the new CLAS polarization observables (see Figs. 2 and 3): F, H, P, and T. Particularly, the predicted target asymmetry appeared to have the wrong sign using the definitions for these observables from Ref. [4].

The BnGa solution for the new CLAS data presented here confirms the five dominant partial wave amplitudes that were reported in Ref. [26]. The $J^P = 3/2^+$ partial wave exhibits a significant peak close to $W = 1800$ MeV that is identified with the $N(1720)\,3/2^+$ resonance. A notable contribution from the $3/2^-$ partial wave is observed above 2 GeV and identified with the $N(2120)\,3/2^-$. Compared with earlier findings, the coupling of the $N(1875)\,3/2^-$ to $N\omega$ has decreased by about 70 %. The intensity appears to have shifted to the $5/2^+$ partial wave above $W = 1900$ MeV, where the contribution of the $N(2000)\,5/2^+$ state has been observed to increase by about 50 %. The $1/2^-$ partial wave exhibits a smoother behavior, but the analysis found that the coupling to $N(1895)\,1/2^-$ has not significantly changed. This smoother behavior is a result of a sign change in the contribution of the non-resonant amplitudes. The dominant contributions, in particular of the $N(2000)\,5/2^+$ state, are consistent with the results of a single-channel PWA by the CLAS Collaboration [30].

The effective Lagrangian approach by Wei *et al.* [23] is based on all published data from the CLAS Collaboration, including the new double-polarization observables discussed here. To achieve a good description of the data, seven nucleon resonances have been added in the analysis. A significant peak in the $3/2^+$ wave around $W = 1800$ MeV is confirmed, which originates from the $N(1720)\,3/2^+$. The $3/2^-$ partial wave shows important contributions, which mainly stem from the $N(1520)\,3/2^-$ and $N(1700)\,3/2^-$ resonances ($W < 2$ GeV), in agreement with the BnGa analysis. The latter two resonances prove to be important in the description of the new F and H observables. This analysis also identifies significant contributions from the $5/2^+$ partial wave, again consistent with the findings of the BnGa group.

In summary, the beam-target double-polarization observables F, P, and H in the reaction $\vec{\gamma}\vec{p} \to p\omega$ have been measured for the first time across the N^* resonance

region. Convergence among different groups on the leading N^* resonance contributions appears imminent based on these new measurements. Several poorly known states have been identified in ω photoproduction. Particularly noteworthy are contributions from the new N^* states that have been listed in the Review of Particle Properties since 2014 based on photoproduction experiments. In the $3/2^-$ partial wave for example, contributions from the recently added $N(1875)\,3/2^-$ and $N(2120)\,3/2^-$ states are observed. Also identified in ω photoproduction is the new $N(1880)\,1/2^+$ state which, together with the $N(1900)\,3/2^+$ and $N(1990)\,7/2^+$ states, and the poorly established $N(2000)\,5/2^+$ state, is considered to form a quartet of nucleon states in the ($\mathbf{70}$, 2_2^+) supermultiplet with quark spin $S = 3/2$ and positive parity. Some open questions remain, including the relative strength of t-channel contributions close to the reaction threshold from the exchange of either pomerons or pions. A full discussion of the contributing N^* resonances, their $N\omega$ couplings, and the impact of particular observables will be available in forthcoming papers [23, 31].

The authors gratefully acknowledge the excellent support of the technical staff at Jefferson Lab and all participating institutions. This research is based on work supported by the U. S. Department of Energy, Office of Science, Office of Nuclear Physics, under Contract No. DE-AC05-06OR23177. The group at Florida State University acknowledges additional support from the U.S. Department of Energy, Office of Science, Office of Nuclear Physics, under Contract No. DE-FG02-92ER40735. This work was also supported by the U. S. National Science Foundation, the State Committee of Science of Republic of Armenia, the Chilean Comisión Nacional de Investigación Cientifica y Tecnológica, the Italian Istituto Nazionale di Fisica Nucleare, the French Centre National de la Recherche Scientifique, the French Commissariat a lEnergie Atomique, the Scottish Universities Physics Alliance (SUPA), the United Kingdom Science and Technology Facilities Council (STFC), the National Research Foundation of Korea, the Deutsche Forschungsgemeinschaft (SFB/TR110), the Russian Science Foundation under Grant No. 16-12-10267, and the National Natural Science Foundation of China under Grants No. 11475181 and No. 11635009.

* Present address: Department of Physics, University of Michigan, Ann Arbor, Michigan 48109,USA
† Present address: Korea Atomic Energy Research Institute, Gyeongju-si, 38180, South Korea
‡ Corresponding author: crede@fsu.edu
§ Present address: Mississippi State University, Mississippi State, MS 39762-5167, USA
¶ Present address: Imam Abdulrahman Bin Faisal University, Industrial Jubail 31961, Saudi Arabia
** Present address: Idaho State University, Pocatello, Idaho 83209, USA
†† Present address: Oak Ridge National Laboratory, Oak Ridge, TN 37831, USA
‡‡ Present address: INFN, Sezione di Genova, 16146 Genova, Italy

[1] E. Klempt and J. M. Richard, Rev. Mod. Phys. **82**, 1095 (2010).
[2] V. Crede and W. Roberts, Rept. Prog. Phys. **76**, 076301 (2013).
[3] I. S. Barker, A. Donnachie and J. K. Storrow, Nucl. Phys. B **95**, 347 (1975).
[4] C. G. Fasano, F. Tabakin and B. Saghai, Phys. Rev. C **46**, 2430 (1992).
[5] M. Pichowsky, C. Savkli and F. Tabakin, Phys. Rev. C **53**, 593 (1996).
[6] Z. Akbar *et al.* [CLAS Collaboration], Phys. Rev. C **96**, no. 6, 065209 (2017).
[7] P. Roy *et al.* [CLAS Collaboration], Phys. Rev. C **97**, no. 5, 055202 (2018).
[8] C. D. Keith *et al.*, Nucl. Instrum. Meth. A **684**, 27 (2012).
[9] P. Roy, Ph.D. thesis, Florida State University, 2016.
[10] H. Olsen and L. C. Maximon, Phys. Rev. **114**, 887 (1959).
[11] D. I. Sober *et al.*, Nucl. Instrum. Meth. A **440**, 263 (2000).
[12] B. A. Mecking *et al.*, Nucl. Instrum. Meth. A **503**, 513 (2003).
[13] M. Williams, M. Bellis and C. A. Meyer, JINST **4**, P10003 (2009).
[14] C. A. Paterson *et al.* [CLAS Collaboration], Phys. Rev. C **93**, no. 6, 065201 (2016).
[15] Y. S. Oh, A. I. Titov and T. S. H. Lee, Phys. Rev. C **63**, 025201 (2001).
[16] Q. Zhao, Phys. Rev. C **63**, 025203 (2001).
[17] A. I. Titov and T. S. H. Lee, Phys. Rev. C **66**, 015204 (2002).
[18] G. Penner and U. Mosel, Phys. Rev. C **66**, 055212 (2002).
[19] V. Shklyar, H. Lenske, U. Mosel and G. Penner, Phys. Rev. C **71**, 055206 (2005) Erratum: [Phys. Rev. C **72**, 019903 (2005)].
[20] P. Collins *et al.* [CLAS Collaboration], Phys. Lett. B **773**, 112 (2017).
[21] A. V. Anisovich and A. V. Sarantsev, Eur. Phys. J. A **30**, 427 (2006).
[22] `https://pwa.hiskp.uni-bonn.de/baryon_x.htm`
[23] N. C. Wei *et al.* (in preparation).
[24] A. C. Wang, W. L. Wang, F. Huang, H. Haberzettl and K. Nakayama, Phys. Rev. C **96**, 035206 (2017).
[25] A. C. Wang, W. L. Wang and F. Huang, Phys. Rev. C **98**, no. 4, 045209 (2018).
[26] I. Denisenko *et al.*, Phys. Lett. B **755**, 97 (2016).
[27] A. Wilson *et al.* [CBELSA/TAPS Collaboration], Phys. Lett. B **749**, 407 (2015).
[28] H. Eberhardt *et al.*, Phys. Lett. B **750**, 453 (2015).
[29] F. Klein *et al.* [CBELSA/TAPS Collaboration], Phys. Rev. D **78**, 117101 (2008).
[30] M. Williams *et al.* [CLAS Collaboration], Phys. Rev. C **80**, 065209 (2009).
[31] A. V. Anisovich *et al.* (in preparation).